CODEN IEJMAT *Internet Electronic Journal of Molecular Design* **2005**, *4*, 556–578 ISSN 1538–6414
BioChem Press http://www.biochempress.com

Inter*net* Electronic Journal of Molecular Design

August 2005, Volume 4, Number 8, Pages 556–578

Editor: Ovidiu Ivanciuc

Special issue dedicated to Professor Danail Bonchev on the occasion of the 65th birthday

1,5–*N*,*N*′–Disubstituted–2–(Substituted Benzenesulphonyl)–Glutamamide Analogues as Anticancer Agents. Part 3. Synthesis, Biological Screening and QSAR Study

Shovanlal Gayen, Bikash Debnath, Soma Samanta, Balaram Ghosh, Anindya Basu, and Tarun Jha

Division of Medicinal and Pharmaceutical Chemistry, Department of Pharmaceutical Technology, P.O. Box 17020, Jadavpur University, Kolkata 700 032, India

Received: November 26, 2004; Revised: March 8, 2005; Accepted: May 2, 2005; Published: August 31, 2005

Citation of the article:
S. Gayen, B. Debnath, S. Samanta, B. Ghosh, A. Basu, and T. Jha, 1,5–*N*,*N*′–Disubstituted–2–(Substituted Benzenesulphonyl)–Glutamamide Analogues as Anticancer Agents. Part 3. Synthesis, Biological Screening and QSAR Study, *Internet Electron. J. Mol. Des.* **2005**, *4*, 556–578, http://www.biochempress.com.

Copyright © 2005 BioChem Press

Inter*net* Electronic Journal of Molecular Design

BioChem Press
http://www.biochempress.com

1,5–*N*,*N*′–Disubstituted–2–(Substituted Benzenesulphonyl)–Glutamamide Analogues as Anticancer Agents. Part 3.† Synthesis, Biological Screening and QSAR Study

Shovanlal Gayen, Bikash Debnath, Soma Samanta, Balaram Ghosh, Anindya Basu, and Tarun Jha *

Division of Medicinal and Pharmaceutical Chemistry, Department of Pharmaceutical Technology, P.O. Box 17020, Jadavpur University, Kolkata 700 032, India

Received: November 26, 2004; Revised: March 8, 2005; Accepted: May 2, 2005; Published: August 31, 2005

Internet Electron. J. Mol. Des. **2005**, *4* (8), 556–578

Abstract

Motivation. Numerous studies on glutamine metabolism in cancer demonstrate that glutamic acid and glutamine analogues may be developed as possible antitumor agents. Efforts were made to synthesize glutamamide analogues, structural variants of glutamic acid and glutamine, contains both the amido groups at 1 and 5 positions of glutamic acid and derivatives of both glutamine and isoglutamine.

Method. Twenty eight new 1,5–*N*,*N*′–disubstituted–2–(substituted benzenesulphonyl) glutamamides were synthesized in continuation to our earlier work. These compounds were screened for antitumor activity and a QSAR study was performed to explore the substitutional requirements for the improved anticancer activity using physicochemical and topological parameters.

Results. The final QSAR model obtained has correlation coefficient, standard error of estimate and cross–validated R^2 of 0.889, 0.068 and 0.697, respectively. This QSAR study showed the importance of particular atoms and identified a functional region of the molecule with the potential as the pharmacophore related with dispersive/van der Waals and electronic interaction with the receptor(s). The study also showed that the increased molar volumes of these analogues have advantageous effect to the antitumor activity.

Conclusions. The study helps to understand the relationship of the chemical structure of this type of compounds with the anticancer activity. The QSAR study may be helpful for further synthesis of highly active glutamamide analogues as antitumor agents.

Keywords. Glutamamide; antitumor agents; synthesis; screening; quantitative structure–activity relationships; QSAR; drug design.

Abbreviations and notations

ETSA, electrotopological state atom	MLR, multiple linear regression
RTSA, refractotopological state atom	QSAR, quantitative structure–activity relationships

† Part 1 and Part 2 were published earlier in *Bioorg. Med. Chem*. **2002**, *10*, 1841– 1854 and *Internet Electron. J. Mol. Des*. **2002**, *1*, 488–502, www.biochempress.com. These are mentioned in this article as refs. [17] and [19], respectively.
# Dedicated on the occasion of the 65th birthday to Danail Bonchev. Presented in part at the Internet Electronic Conference of Molecular Design 2004, IECMD 2004.
* Correspondence author; phone: 91–33–2414 6677; mobile: 09433187443; fax: 91–33–2414 6677/91–33–2414 6927; E–mail: tjjupharm@yahoo.com, tarunjha123@yahoo.co.in.

1 INTRODUCTION

Tumors have been described as nitrogen traps [1,2]. They require a continuous supply of both essential and nonessential amino acids as nitrogen source for increased biosynthesis of nucleic acids and proteins – the two most essential components of genomics and proteomics. Glutamine (**1**) is the most abundant free amino acid in the human body and, therefore, plays a key role in tumor cell growth by supplying its amide nitrogen atoms in the biosynthesis of other amino acids, purine and pyrimidine bases [3] via a family comprised of 16 amidotransferases with diversified mechanisms [4,5]. It is one of the two, if not the only, major substrate of cancer [6]. Thus, tumors indeed behave as glutamine (**1**) traps. The tumor growth causes a change in host glutamine (**1**) metabolism so that host nitrogen metabolism is accommodated to the tumor–enhanced requirements of glutamine (**1**) [7–9]. To be used in this process, glutamine (**1**) must reach into mitochondria of tumor cells through plasma membrane and inner mitochondrial membrane transporters. Glutamine (**1**) also plays an important function in multiple metabolic pathways and an important component in the cell culture media for both carbon and nitrogen source [10]. All of the tumor cells studied so far had a high activity of phosphate–dependent glutaminase [11]. These were found to utilize glutamine (**1**) from the culture medium during long–term culture. Rates of cell growth, DNA and protein synthesis as well as thymidine transport were correlated with the glutamine (**1**) concentration in the culture media [11]. Patients of cancer often develop muscle glutamine (**1**) depletion due to uptake by tumors and chronic protein catabolism [6]. Cell growth is a function of glutamine (**1**) influx and suggests that glutamine (**1**) is used to supply glutamate and cystine perhaps for glutathione synthesis [12]. The reported antagonists of glutamine (**1**) *eg*. Azaserine (**2**), 6–diaza–5–oxo–L–norleucin (DON) (**3**) and Acivicin (**4**), which are shown in Figure 1, are potent inhibitors of glutamine (**1**) dependent amidotransferases [13]. These observations support our rationale for the synthesis of the title compounds. In keeping all these points in view, it was assumed that structural variants of glutamine (**1**) and the biotransformation product glutamic acid might possess antitumor activity.

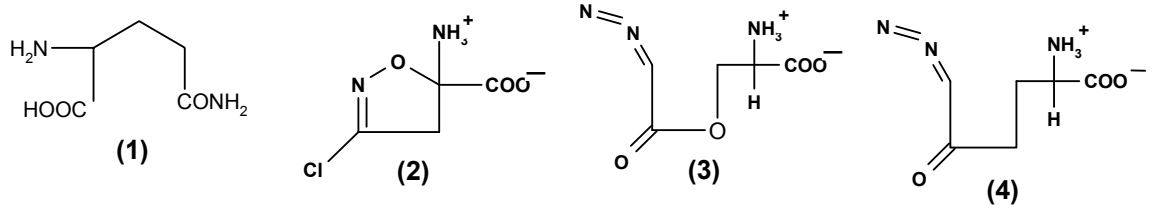

Figure 1. Structure of glutamine (**1**), azaserine (**2**), DON (**3**) and acivicin (**4**).

In the present study, some glutamamide analogues, which are structural variants of glutamine (**1**) as well as glutamic acid, were synthesized and biologically evaluated for their antitumor activity as a part of our composite programme of rational drug design [14–30]. QSAR study was performed to find out the structural requirements of glutamamide analogues for antitumor activity.

2 MATERIALS AND METHODS

2.1 Synthesis

Synthesis of 1,5–*N*,*N*′–disubstituted–2–(substituted benzenesulphonyl) glutamamides (**10–37**) was carried out as presented in Scheme 1.

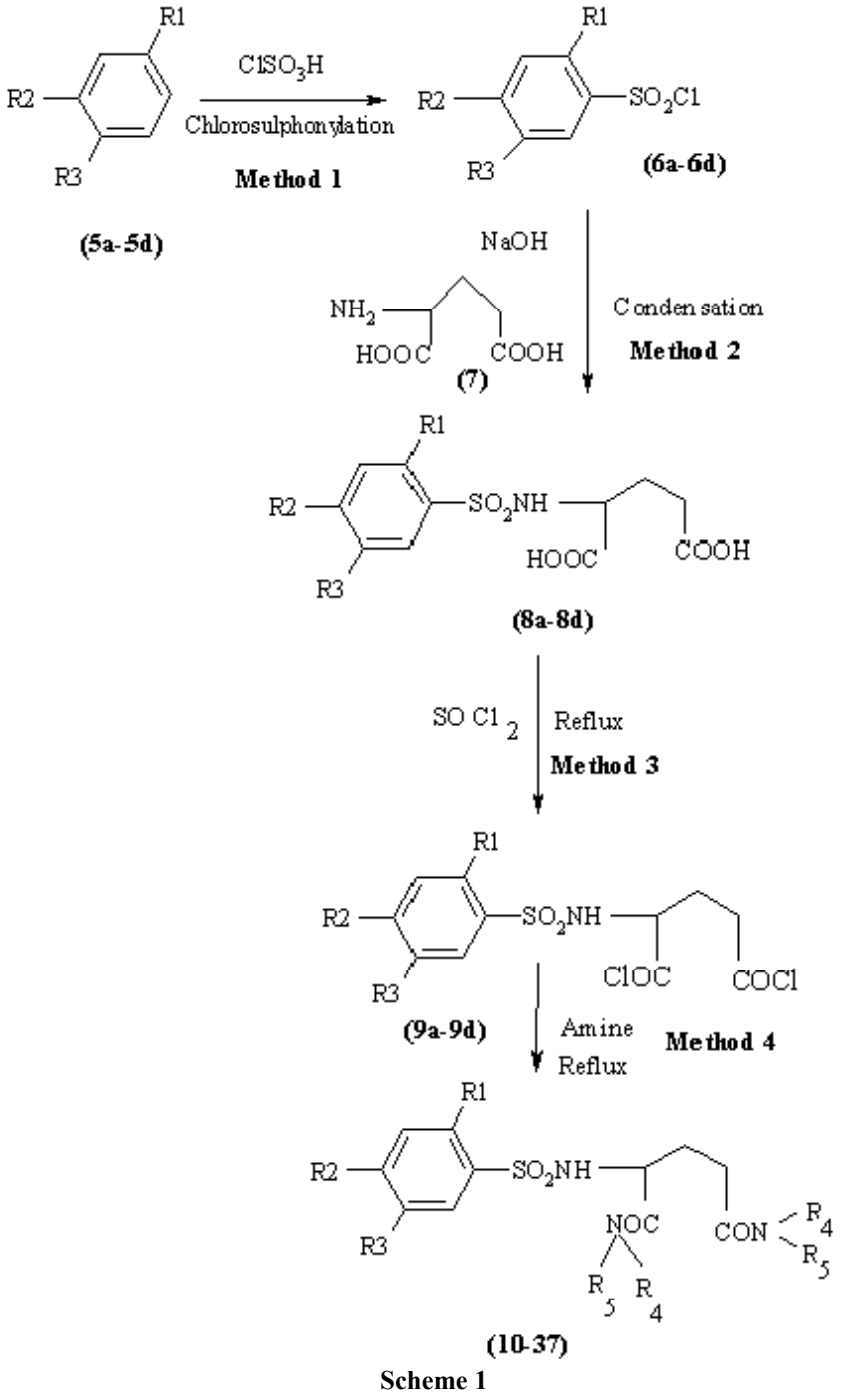

Scheme 1

2.1.1 Chemistry

Synthesis of 1,5–*N*,*N*′–disubstituted–2–(substituted benzenesulphonyl) glutamamides (**10–37**) (Figure 2) was carried out according to Scheme 1. Synthesis was started with chlorosulphonylation

of substituted benzenes (**5**), to get corresponding sulphonyl chlorides (**6**). These halides (**6**) prove to be versatile synthons in the subsequent step for the preparation of substituted benzenesulphonyl glutamic acids (**8**). 2–(Substituted benzenesulphonyl) glutamic acids (**8**) were prepared by one–step Schotten–Bauman condensation (Method 2) with L–glutamic acid (**7**). In this reaction alkaline medium was maintained to remove the hydrochloric acid, which is formed during condensation. Reaction of resulting intermediates (**8**), with thionyl chloride afforded the acyl chlorides, 2–(substituted benzenesulphonyl) glutamic acid dichlorides (**9**). By a nucleophillic displacement of intermediate with amines (amino–dehydroxylation) we obtained the corresponding amides (**10–37**). Commercially available reagents and starting materials were obtained from Sigma, Qualigens, Glaxo, Fluka, Merck, Ranbaxy and were used with no additional purification.

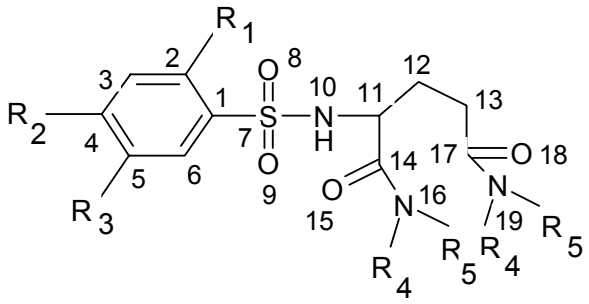

Figure 2. General structure of glutamamide analogs with arbitrary numbering of common atoms.

2.1.2 General Synthetic Procedures

Method 1. **Substituted benzenesulphonyl chlorides** (**6a–6d**). To a mixture of substituted benzene (0.1 mole) in chloroform (50 ml) in a 500 ml flask equipped with a dropping funnel, a thermometer and a reflux condenser, chlorosulphonic acid (0.25 mole) was added drop–wise over a period of 45 min to 60 min. The reaction mixture was magnetically stirred at 0°C in a bath containing freezing mixture of ice and salt. Chlorosulphonic acid was added in such a rate that the temperature of the reaction mixture does not exceed 5°C. After the complete addition of chlorosulphonic acid, the reaction mixture was stirred for another 45 min at room temperature and the mixture was poured on to crushed ice. The product was extracted with three 50–ml portions of chloroform, dried overnight over anhydrous sodium sulphate. Chloroform was distilled off. The product (**6a–6d**) was sufficiently pure which was not attempted for further purification. It has been taken for the next step.

Method 2. **2–(Substituted benzenesulphonyl) glutamic acids** (**8a–8d**). L–glutamic acid 8 (14.7 g: 0.1 mole) was taken in a 250 ml conical flask and sodium hydroxide solution (2N) was added slowly till all the glutamic acid dissolves and mixture becomes distinctly alkaline to phenolphthalein. The reaction mixture was stirred on the mechanical stirrer with temperature maintained at 95–100 °C using hot water bath. Substituted benzenesulphonyl chloride (0.15 moles) was added in small portions with constant stirring and time–to–time addition of sodium hydroxide

solution (2N) to keep the reaction mixture alkaline. The reaction was continued until a clear homogeneous solution results or the thin layer chromatography showed the reaction to be complete. After the reaction was over, it was allowed to cool to room temperature and filtered to separate undissolved solid matter if any. The filtrate was acidified with concentrated hydrochloric acid and saturated with sodium chloride. The product was extracted with three 50 ml portions of ethyl acetate. Ethyl acetate layer was washed with brine solution (15 ml) and dried overnight over anhydrous sodium sulphate. The solvent was distilled off to get the product. The product (8a–8d) obtained was not attempted further purification step to avoid undesirable degradation.

Method 3. **2–(substituted benzenesulphonyl)–glutamic acid dichloride** (**9a–9d**). 2–(Substituted benzene sulphonyl) glutamic acid (8a–8d) (0.01 mole) was taken in 100 ml round bottomed flask fitted with reflux condenser and calcium chloride guard tube. Thionyl chloride (0.025 mole) was added to it and refluxed for 1 h on boiling water bath with occasional stirring. The reaction mixture was further heated for additional 30 min or until the evolution of HCl gas ceases. The completion of the reaction was tested by thin layer chromatography. After the reaction was completed, the reaction mixture was cooled to room temperature. The apparatus was then rearranged and the excess of thionyl chloride was removed by distillation with three 10 ml portions of dry benzene under reduced pressure. The resultant dichloride (9a–9d) was sufficiently pure for the subsequent reactions and hence, to avoid unnecessary decomposition, further purification was not attempted.

Method 4. **1,5–*N*,*N*′–disubstituted 2–(substituted benzenesulphonyl) glutamamides** (**10–37**). A 50–mL round–bottomed flask containing 2–(substituted benzenesulphonyl)– 1,5–dicarboxylic acid dichloride (**9a–9d**) (1 equivalent) in 10 ml of dry benzene was fitted with reflux condenser. Acyl chloride was added with excess of amine (2.5 equivalent) and refluxed on the water bath for 30 min or until the evolution of hydrochloric gas ceases. Benzene and traces of unreacted amine were removed by heating the flask in water bath. It was then filtered at the pump and recrystallized from dilute ethanol.

2.1.3 Characterization

Melting points were measured on a capillary melting point apparatus and were uncorrected. All the compounds were characterized qualitatively and quantitatively by performing both analytical and spectrophotometric analysis. The infrared spectra were recorded on BUCK M500 quick scanning Infrared spectrophotometer using KBr pellets. Running the spectrum of 0.05mm polystyrene film did the finer calibration of the machine. The frequencies were expressed in cm^{-1}. Proton nuclear magnetic resonance (^1H NMR) spectra were collected at 25°C in the pulsed Fourier Transformation mode on Bruker DRX 500 or Bruker DRX 300 MHz spectrophotometers using the solvents described and was consistent with the proposed structures. Chemical shifts are reported in δ ppm (parts per million) relative to tetramethyl silane for deuterated dimethylsulfoxide (DMSO–

d_6). Signals are quoted as s (singlet), d (doublet), t (triplet), q (quartet) and m (multiplet). The mass spectra (FAB) were recorded on JEOL–JMS–SX–PNBA. *p*–Nitrobenzyl alcohol was used as matrix (M^+) which showed M+1 peak at 154, 2M+1 peak at 307. Elemental or microanalysis (C, H, N) of the compounds was performed on 2400 Series II CHN analyzer of Perkin–Elmer. Physical data of intermediate compounds are shown in Table 1 and that of final compounds are shown in Table 2 respectively. Mass–, IR–, and Proton NMR spectroscopic as well as microanalysis data of the final compounds (**10–37**) are shown in Table 3.

Table 1. Physical Data for the Intermediate Compounds

Cpd [a]	R_1	R_2	R_3	Mp (°C) [b]	% Yield	Molecular formula	MW [c]
6a	H	Cl	H	44–45	82.42	$C_6H_4Cl_2O_2S$	211.07
7b	Cl	H	Cl	Liquid	62.36	$C_6H_3Cl_3O_2S$	245.51
6c	H	*i*–C_4H_9	H	Liquid	78.82	$C_{10}H_{13}ClO_2S$	232.73
6d	H	*t*– C_4H_9	H	56–58	71.61	$C_{10}H_{13}ClO_2S$	232.73
8a	H	Cl	H	115–116	64.23	$C_{11}H_{12}ClNO_6S$	321.74
8b	Cl	H	Cl	156–158	42.51	$C_{11}H_{11}ClNO_6S$	356.18
8c	H	*i*–C_4H_9	H	205–206	73.42	$C_{15}H_{21}NO_6S$	343.40
8d	H	*t*– C_4H_9	H	162–164	43.84	$C_{15}H_{21}NO_6S$	343.40

[a] Compound number; [b] Melting point; [c] Molecular weight

Table 2. Physical Data of Synthesized Glutamamide Analogues (**10–37**)

Cpd [a]	R_1	R_2	R_3	R_4	R_5	Mp (°C) [b]	% Yield	Molecular formula	MW [c]
10	H	Cl	H	H	H	206–208	84.34	$C_{11}H_{14}ClN_3O_4S$	319.76
11	H	Cl	H	CH_3	H	230–232	72.54	$C_{13}H_{18}ClN_3O_4S$	347.82
12	H	Cl	H	C_2H5	H	220–222	81.64	$C_{15}H_{22}ClN_3O_4S$	375.87
13	H	Cl	H	*n*–C_3H_7	H	218–220	83.21	$C_{17}H_{26}ClN_3O_4S$	403.93
14	H	Cl	H	*i*– C_3H_7	H	138–140	78.56	$C_{17}H_{26}ClN_3O_4S$	403.93
15	H	Cl	H	*n*–C_4H_9	H	130–132	86.71	$C_{19}H_{30}ClN_3O_4S$	431.98
16	H	Cl	H	*i*– C_4H_9	H	162–164	84.43	$C_{19}H_{30}ClN_3O_4S$	431.98
17	H	Cl	H	CH3	CH3	142–144	77.86	$C_{15}H_{22}ClN_3O_4S$	375.87
18	H	Cl	H	C_6H_5	H	135–137	69.53	$C_{23}H_{22}ClN_3O_4S$	471.96
19	H	Cl	H	C_2H_5	C_2H_5	146–148	80.56	$C_{19}H_{30}ClN_3O_4S$	431.98
20	H	Cl	H	*n*–C_6H_{13}	H	188–190	68.36	$C_{23}H_{38}ClN_3O_4S$	488.08
21	Cl	H	Cl	H	H	152–154	73.89	$C_{11}H_{13}Cl_2N_3O_4S$	354.21
22	Cl	H	Cl	CH3	H	170–172	65.62	$C_{13}H_{17}Cl_2N_3O_4S$	382.26
23	Cl	H	Cl	*n*– C_3H_7	H	144–146	72.65	$C_{17}H_{25}Cl_2N_3O_4S$	438.37
24	Cl	H	Cl	c–C_6H_{11}	H	195–197	68.31	$C_{23}H_{33}Cl_2N_3O_4S$	518.50
25	H	*i*– C_4H_9	H	H	H	150–152	70.24	$C_{15}H_{23}N_3O_4S$	341.43
26	H	*i*– C_4H_9	H	CH_3	H	125–127	65.21	$C_{17}H_{27}N_3O_4S$	369.48
27	H	*i*– C_4H_9	H	C_2H_5	H	141–143	67.83	$C_{19}H_{31}N_3O_4S$	397.53
28	H	*i*– C_4H_9	H	*n*– C_3H_7	H	143–145	61.57	$C_{21}H_{35}N_3O_4S$	425.59
29	H	*i*– C_4H_9	H	*i*– C_3H_7	H	132–134	62.31	$C_{21}H_{35}N_3O_4S$	425.59
30	H	*i*– C_4H_9	H	n– C_4H_9	H	139–141	71.90	$C_{23}H_{39}N_3O_4S$	453.64
31	H	*i*– C_4H_9	H	*i*– C_4H_9	H	136–138	73.74	$C_{23}H_{39}N_3O_4S$	453.64
32	H	*i*– C_4H_9	H	C_6H_5	H	168–170	62.41	$C_{27}H_{31}N_3O_4S$	493.62
33	H	*i*– C_4H_9	H	CH_3	CH3	162–164	51.24	$C_{19}H_{31}N_3O_4S$	397.53
34	H	*i*– C_4H_9	H	*c*–C_6H_{11}	H	196–198	83.21	$C_{27}H_{43}N_3O_4S$	505.74
35	H	*i*– C_4H_9	H	*n*–C_6H_{13}	H	175–177	73.48	$C_{27}H_{47}N_3O_4S$	509.75
36	H	*t*– C_4H_9	H	CH_3	H	178–180	64.53	$C_{17}H_{27}N_3O_4S$	369.48
37	H	*t*– C_4H_9	H	C_2H_5	C_2H_5	183–185	69.72	$C_{23}H_{39}N_3O_4S$	453.64

[a] Compound number; [b] Melting point; [c] Molecular weight

Table 3. Mass–, IR– and Proton NMR Spectroscopic as well as CHN Analysis Data of the Final Compounds (**10–37**)

Cpd	Mass (FAB)	IR (KBr, cm^{-1})	^{1}HNMR (300 MHz, DMSO–d_6)	C,H,N: calcd/found		
				C	H	N
10	M + H^+ peak at m/z 320.	3350 (N–H str of CONH), 3078 (Ar–C–H str), 2938 (ali–C–H str), 1640, 1562, 1470 (ali C–H def), 1355 (S=O str of SO_2NH, asymmetric), 1259 (S=O str of SO_2NH, symmetric), 972, 890 (Ar–C–H def)	7.86 (d, 2H, H–2', H–6'), 7.76 (d, 2H, H–3', H–5'), 7.48 (s, 1H, SO_2NH), 7.38 (m, 2H, $CONH_2$–1), 7.10 (m, 2H, $CONH_2$–5), 3.64 (m, 1H, H–2), 2.46–1.96 (m, 4H, H_2–3, H_2–4)	41.32 41.46	4.91 4.89	13.14 13.21
11	M + H^+ peak at m/z 348	3348 (N–H str of CONH), 3086 (Ar–C–H str), 2940 (ali C–H str), 1652, 1567, 1482 (ali C–H def), 1348 (S=O str of SO_2NH, asymmetric), 1262 (S=O str of SO_2NH, symmetric), 1021, 978, 896 (Ar–C–H def)	7.83 (d, 2H, H–2', H–6'), 7.75 (d, 2H, H–3', H–5'), 7.52 (s, 1H, SO_2NH), 7.32 (m, 1H, CONH–1), 7.19 (m, 1H, CONH–5), 3.57 (m, 1H, H–2), 2.62 (t, 3H, N–CH_3–1'"), 2.34 (m, 3H, N–CH_3–1"), 2.03–1.67 (m, 4H, H_2–3, H_2–4)	44.89 44.71	5.22 5.19	12.08 12.18
12	M + H^+ peak at m/z 376	3346 (N–H str of CONH), 3082 (Ar–C–H str), 2934 (ali C–H str), 1640, 1548, 1485 (ali C–H def), 1354 (S=O str of SO_2NH, asymmetric), 1264 (S=O str of SO_2NH, symmetric), 1026, 982, 896 (Ar–C–H def)	7.85 (d, 2H, H–2', H–6'), 7.78 (d, 2H, H–3', H–5'), 7.50 (s, 1H, SO_2NH), 7.29 (m, 1H, CONH–1), 7.21 (m, 1H, CONH–5), 3.54 (m, 1H, H–2), 3.07 (m, 2H, N–CH_2–1") 2.91 (m, 2H, N–CH_2–1'"), 2.21 (m, 2H, H_2–4), 1.74 (m, 2H, H_2–3), 1.16 (m, 3H, CH_3–2'") 1.02 (m, 3H, CH_3–2")	47.93 47.76	5.90 5.88	11.18 11.14
13	M + H^+ peak at m/z 405	3350 (N–H str of CONH), 3082 (Ar–C–H str), 2935 (ali C–H str), 1652, 1568, 1478 (ali C–H def), 1358 (S=O str of SO_2NH, asymmetric), 1272 (S=O str of SO_2NH, symmetric), 1018, 972, 888 (Ar–C–H def)	7.96 (d, 2H, H–2', H–6'), 7.82 (d, 2H, H–3', H–5'), 7.65 (s, 1H, SO_2NH), 7.19 (m, 1H, CONH–1), 7.13 (m, 1H, CONH–5), 3.65 (m, 2H, N–CH_2–1") 3.13 (m, 2H, N–CH_2–1'"), 2.98 (m, 1H, H–2), 2.78 (m, 2H, H_2–4), 2.03 (m, 2H, H_2–3), 1.35 (m, 2H, CH_2–2") 1.24 (m, 2H, CH_2–2'"), 1.08 (m, 3H, CH_3–3"), 0.79 (m, 3H, CH_3–3'")	50.55 50.62	6.49 6.46	10.40 10.43
14	M + H^+ peak at m/z 405	3356 (N–H str of CONH), 3084 (Ar–C–H str), 2942 (ali C–H str), 1650, 1562, 1472 (ali C–H def), 1346 (S=O str of SO_2NH, asymmetric), 1268 (S=O str of SO_2NH, symmetric), 976, 896 (Ar–C–H def)	8.02 (d, 2H, H–2', H–6'), 7.84 (d, 2H, H–3', H–5'), 7.60 (s, 1H, SO_2NH), 7.32 (m, 1H, CONH–1), 7.06 (m, 1H, CONH–5), 3.49 (m, 1H, N–CH–1'"), 3.17 (m, 1H, N–CH–1"), 3.13 (m, 1H, H–2), 1.94 (m, 2H, H_2–3), 2.64 (m, $2H_2$, H–4), 1.22–1.11 (m, 6H, CH_3–2", CH_3–3"), 0.98–0.84 (m, 6H, CH_3–2'", CH_3–3'")	50.55 50.54	6.49 6.50	10.50 10.58
15	M + H^+ peak at m/z 433	3344 (N–H str of CONH), 3082 (Ar–C–H str), 2934 (ali C–H str), 1640, 1560, 1484 (ali C–H def), 1353 (S=O str of SO_2NH, asymmetric), 1272 (S=O str of SO_2NH, symmetric), 1024, 978, 896 (Ar–C–H def)	7.92 (d, 2H, H–2', H–6'), 7.78 (d, 2H, H–3', H–5'), 7.65 (s, 1H, SO_2NH), 7.43 (m, 1H, CONH–1), 7.17 (m, 1H, CONH–5), 3.52 (m, 2H, N–CH_2–1") 3.45 (m, 1H, H–2), 3.18 (m, 2H, N–CH_2–1'"), 2.57 (m, 2H, H_2–4) 1.92 (m, 2H, H_2–3), 1.35–1.06 (m, 8H, CH_2–2", CH_2–3", CH_2–2'", CH_2–3'") 0.95–0.82 (m, 6H, CH_3–4", CH_3–4'")	52.83 52.74	7.00 6.98	9.73 9.82

Table 3. (Continued)

Cpd	Mass (FAB)	IR (KBr, cm^{-1})	^{1}HNMR (300 MHz, DMSO–d_6)	C,H,N: %calcd/found		
				C	H	N
16	M + H^+ peak at m/z 433	3350 (N–H str of CONH), 3078, (Ar–C–H str), 2944 (ali C–H str), 1644, 1553, 1487 (ali C–H def), 1348 (S=O str of SO_2NH, asymmetric), 1262 (S=O str of SO_2NH, symmetric), 978, 892 (Ar–C–H def)	7.88 (d, 2H, H–2', H–6'), 7.75 (d, 2H, H–3', H–5'), 7.48 (s, 1H, SO_2NH), 7.42 (m, 1H, CONH–1), 7.25 (m, 1H, CONH–5), 3.62 (m, 1H, H–2), 3.39 (m, 2H, N–CH_2–1"), 3.17 (m, 2H, N–CH_2–1'"), 2.56 (m, 2H, H_2–4), 1.97 (m, 2H, H_2–3), 1.23–0.87 (m, 14H, CH–2", CH–2'", CH_3–3", CH_3–3'", CH_3–4", CH_3–4'")	52.83 52.76	7.00 6.99	9.73 9.72
17	M + H^+ peak at m/z 377	3366 (N–H str of CONH), 3092 (Ar–C–H str), 2946 (ali C–H str), 1652, 1574, 1487 (ali C–H def), 1356 (S=O str of SO_2NH, asymmetric), 1274 (S=O str of SO_2NH, symmetric), 1026, 986, 898 (Ar–C–H def)	7.98 (s, 1H, SO_2NH), 7.95 (d, 2H, H–2', H–6'), 7.73 (d, 2H, H–3', H–5'), 3.26 (m, 6H, CH_3–1", CH_3–2") 3.16 (m, 1H, H–2), 2.86 (m, 6H, CH_3–1'", CH_3–2'"), 2.28 (m, 2H, H_2–4), 2.04 (m, 2H, H_2–3)	47.93 47.96	5.90 5.91	11.18 11.12
18	MS (FAB): M + H^+ peak at m/z 473	3358 (N–H str of CONH), 3094 (Ar–C–H str), 2944 (ali C–H str), 1644, 1562, 1476 (ali C–H def), 1354 (S=O str of SO_2NH, asymmetric), 1262 (S=O str of SO_2NH, symmetric), 1020, 974, 890 (Ar–C–H def)	8.13 (s, 1H, SO_2NH), 7.69 (d, 2H, H–2', H–6'), 7.58 (d, 2H, H–3', H–5'), 7.06–6.87 (m, 10H, phenyl protons), 7.34–7.28 (m, 2H, CONH–1, CONH–5), 2.89 (m, 1H, H–2), 2.41–2.36 (m, 4H, H_2–3, H_2–4)	58.53 58.42	4.70 4.68	8.90 8.86
19	M + H^+ peak at m/z 433	3362 (N–H str of CONH), 3090 (Ar–C–H str), 2938 (ali C–H str), 1640, 1558, 1470 (ali C–H def), 1344 (S=O str of SO_2NH, asymmetric), 1260 (S=O str of SO_2NH, symmetric), 1032, 986, 898 (Ar–C–H def)	8.16 (s, 1H, SO_2NH), 7.89 (d, 2H, H–2', H–6'), 7.64 (d, 2H, H–3', H–5'), 3.37 (m, 1H, H–2), 3.31–3.16 (m, 8H, N–CH_2–1", N–CH_2–3", N–CH_2–1'", N–CH_2–3'"), 2.43 (m, 2H, H_2–4), 2.30 (m, 2H, H_2–3), 1.41 (m, 6H, CH_3–2'", CH_3–4'") 1.32 (m, 6H, CH_3–2", CH_3–4")	52.83 52.76	7.00 7.01	9.73 9.76
20	M + H^+ peak at m/z 489	3346 (N–H str of CONH), 3082 (Ar–C–H str), 2938 (ali C–H str), 1642, 1560, 1472 (ali C–H def), 1346 (S=O str of SO_2NH, asymmetric), 1264 (S=O str of SO_2NH, symmetric), 974, 886 (Ar–C–H def)	7.82 (d, 2H, H–2', H–6'), 7.71 (d, 2H, H–3', H–5'), 7.58 (s, 1H, SO_2NH), 6.84 (d, 1H, CONH–1) 6.66 (d, 1H, CONH–5), 3.36 (m, 2H, N–CH_2–1"), 3.23–3.17 (m, 2H, N–CH_2–1'"), 3.02 (m, 1H, H–2), 2.71 (m, 2H, H_2–3) 2.28(m, 2H, H_2–4), 1.76–1.38 (m, 16H, CH_2–2", CH_2–2'", CH_2–3", CH_2–3'", CH_2–4", CH_2–4'", CH_2–5", CH_2–5'"), 1.08–0.96 (m, 6H, CH_3–6", CH_3–6'")	56.60 56.71	7.85 7.84	8.61 8.64
21	M + H^+ peak at m/z 355	3352 (N–H str of CONH), 3084 (Ar–C–H str), 2944 (ali–C–H str), 1648, 1566, 1482 (ali C–H def), 1354 (S=O str of SO_2NH, asymmetric), 1272 (S=O str of SO_2NH, symmetric), 1024, 978, 896 (Ar–C–H def)	7.98 (d, 1H, H–6'), 7.88 (d, 2H, H–3', H–4'), 7.56 (s, 1H, SO_2NH), 7.42 (m, 2H, $CONH_2$–1), 7.22 (m, 2H, $CONH_2$–5), 3.58 (m, 1H, H–2), 2.36–1.96 (m, 4H, H_2–3, H_2–4)	37.30 37.27	3.70 3.73	11.86 11.87

Table 3. (Continued)

Cpd	Mass (FAB)	IR (KBr, cm^{-1})	^{1}HNMR (300 MHz, DMSO–d_6)	C,H,N: %calcd/found		
				C	H	N
22	$M + H^+$ peak at m/z 383	3354 (N–H str of CONH), 3082 (Ar–C–H str), 2952 (ali C–H str), 1644, 1572, 1478 (ali C–H def), 1355 (S=O str of SO_2NH, asymmetric), 1266 (S=O str of SO_2NH, symmetric), 1022, 974, 892 (Ar–C–H def)	8.04 (d, 1H, H–6'), 7.92 (d, 2H, H–3', H–4'), 7.62 (s, 1H, SO_2NH), 7.38 (m, 1H, CONH–1), 7.26 (m, 1H, CONH–5), 3.62 (m, 1H, H–2), 2.76 (m, 3H, N–CH_3–1"), 2.20 (m, 3H, N–CH_3–1'"), 2.00–1.76 (m, 4H, H_2–3, H_2–4)	40.85 40.73	4.48 4.48	10.99 10.94
23	$M + H^+$ peak at m/z 439	3356 (N–H str of CONH), 3092 (Ar–C–H str), 2948 (ali C–H str), 1648, 1568, 1482 (ali C–H def), 1358 (S=O str of SO_2NH, asymmetric), 1274 (S=O str of SO_2NH, symmetric), 1025, 980, 896 (Ar–C–H def)	7.84 (d, 1H, H–6'), 7.72 (d, 2H, H–3', H–5'), 7.62 (s, 1H, SO_2NH), 7.26 (m, 1H, CONH–1), 7.10 (m, 1H, CONH–5), 3.52 (m, 2H, N–CH_2–1'") 3.22 (m, 2H, N–CH_2–1"), 3.04 (m, 1H, H–2), 2.72 (m, 2H, H–4), 1.98 (m, 2H, H–3), 1.31 (m, 2H, CH_2–2'") 1.18 (m, 2H, CH_2–2"), 1.02 (t, 3H, CH_3–3'"), 0.85 (t, 3H, CH_3–3")	46.58 46.59	5.75 5.74	9.59 9.52
24	$M + H^+$ peak at m/z 519	3366 (N–H str of CONH), 3096 (Ar–C–H str), 2946 (ali C–H str), 1640, 1560, 1482 (ali C–H def), 1354 (S=O str of SO_2NH, asymmetric), 1272 (S=O str of SO_2NH, symmetric), 974, 890 (Ar–C–H def)	7.98 (d, 1H, H–6'), 7.82 (d, 2H, H–3', H–5'), 7.68 (s, 1H, SO_2NH), 7.35 (m, 1H, CONH–1), 7.18 (m, 1H, CONH–5), 3.00 (m, 1H, H–2), 2.76 (m, 2H, H_2–4), 1.92 (m, 2H, H_2–3), 1.56–0.78 (m, 22H, cyclohexyl protons).	53.28 53.32	6.42 6.41	8.10 8.21
25	$M + H^+$ peak at m/z 342	3355 (N–H str of CONH), 3082 (Ar–C–H str), 2938 (ali–C–H str), 1644, 1562, 1482 (ali C–H def), 1354 (S=O str of SO_2NH, asymmetric), 1266 (S=O str of SO_2NH, symmetric), 978, 898 (Ar–C–H def)	7.95 (d, 2H, H–2', H–6'), 7.82 (d, 2H, H–3', H–5'), 7.55 (s, 1H, SO_2NH), 7.44 (m, 2H, $CONH_2$–1), 7.24 (m, 2H, $CONH_2$–5), 3.76 (m, 1H, H–2), 2.90 (m, 2H, CH_2 of Ar–i–Butyl), 2.75 (s, 1H, CH of Ar–i–Butyl), 2.52–1.98 (m, 4H, H_2–3, H_2–4), 1.80–1.65 (m, 6H, two CH_3 of Ar–i–Butyl)	52.77 52.66	6.79 6.81	12.31 12.33
26	$M + H^+$ peak at m/z 370	3350 (N–H str of CONH), 3094 (Ar–C–H str), 2944 (ali C–H str), 1656, 1572, 1484 (ali C–H def), 1365 (S=O str of SO_2NH, asymmetric), 1275 (S=O str of SO_2NH, symmetric), 1032, 982, 896 (Ar–C–H def)	7.92 (d, 2H, H–2', H–6'), 7.78 (d, 2H, H–3', H–5'), 7.48 (s, 1H, SO_2NH), 7.30 (m, 1H, CONH–1), 7.15 (m, 1H, CONH–5), 3.62 (m, 1H, H–2), 2.95 (m, 2H, CH_2 of Ar–i–Butyl), 2.82 (s, 1H, CH of Ar–i–Butyl), 2.56 (m, 3H, N–CH_3–1'"), 2.32 (m, 3H, N–CH_3–1"), 1.93–1.72 (m, 4H, H_2–3, H_2–4) 1.50–1.32 (m, 6H, two CH_3 of Ar–i–Butyl)	55.26 55.34	7.37 7.38	11.37 11.41
27	$M + H^+$ peak at m/z 398	3362 (N–H str of CONH), 3094 (Ar–C–H str), 2936 (ali C–H str), 1640, 1558, 1474 (ali C–H def), 1354 (S=O str of SO_2NH, asymmetric), 1274 (S=O str of SO_2NH, symmetric), 1021, 974, 894 (Ar–C–H def)	7.96 (d, 2H, H–2', H–6'), 7.80 (d, 2H, H–3', H–5'), 7.62 (s, 1H, SO_2NH), 7.42 (m, 1H, CONH–1), 7.26 (m, 1H, CONH–5), 3.58 (m, 1H, H–2), 3.10 (m, 2H, N–CH_2–1'"), 2.96 (m, 2H, CH_2 of Ar–i–Butyl), 2.88 (m, 2H, N–CH_2–1"), 2.75 (s, 1H, CH of Ar–i–Butyl), 2.20 (m, 2H, H_2–4), 1.84 (m, 2H, H_2–3), 1.72–1.55 (m, 6H, two CH_3 of Ar–i–Butyl), 1.22 (t, 3H, CH_3–2'"), 0.92 (m, 3H, CH_3–2")	57.40 57.46	7.86 7.84	10.57 10.61

Table 3. (Continued)

Cpd	Mass (FAB)	IR (KBr, cm^{-1})	^{1}HNMR (300 MHz, DMSO–d_6)	C,H,N: %calcd/found		
				C	H	N
28	M + H^+ peak at m/z 426	3350 (N–H str of CONH), 3092 (Ar–C–H str), 2938 (ali C–H str), 1644, 1562, 1484 (ali C–H def), 1350 (S=O str of SO_2NH, asymmetric), 1268 (S=O str of SO_2NH, symmetric), 978, 898 (Ar–C–H def)	7.88 (d, 2H, H–2', H–6'), 7.76 (d, 2H, H–3', H–5'), 7.58 (s, 1H, SO_2NH), 7.24 (m, 1H, CONH–1), 7.18 (m, 1H, CONH–5), 3.50 (m, 2H, N–CH_2–1'''), 3.20 (m, 2H, N–CH_2–1''), 2.92 (m, 1H, H–2), 2.82 (m, 2H, CH_2 of Ar–i–Butyl), 2.76 (s, 1H, CH of Ar–i–Butyl), 2.62 (m, 2H, H_2–4), 2.00 (m, 2H, H_2–3), 1.78–1.62 (m, 6H, two CH_3 of Ar–i–Butyl), 1.26 (m, 2H, CH_2–2'''), 1.18 (m, 2H, CH_2–2''), 1.00 (m, 3H, CH_3–3'''), 0.68 (m, 3H, CH_3–3'')	59.27 59.36	8.29 8.31	9.87 9.74
29	M + H^+ peak at m/z 426	IR (KBr, cm^{-1}): 3364 (N–H str of CONH), 3086 (Ar–C–H str), 2946 (ali C–H str), 1648, 1566, 1478 (ali C–H def), 1356 (S=O str of SO_2NH, asymmetric), 1270 (S=O str of SO_2NH, symmetric), 1028, 982, 890 (Ar–C–H def)	7.92 (d, 2H, H–2', H–6'), 7.80 (d, 2H, H–3', H–5'), 7.64 (s, 1H, SO_2NH), 7.44 (m, 1H, CONH–1), 7.16 (m, 1H, CONH–5), 3.52 (m, 1H, N–CH–1'''), 3.22 (m, 1H, N–CH–1''), 3.14 (m, 1H, H–2), 2.92 (m, 2H, CH_2 of Ar–i–Butyl), 2.74 (s, 1H, CH of Ar–i–Butyl), 2.62 (m, 2H, H_2–4), 1.88 (m, 2H, H_2–3), 1.70–1.52 (m, 6H, two CH_3 of Ar–i–Butyl), 1.20–1.06 (m, 6H, CH_3–2''', CH_3–3'''), 0.92–0.76 (m, 6H, CH_3–2'', CH_3–3'')	59.27 59.38	8.29 8.30	9.87 9.98
30	M + H^+ peak at m/z 454	3358 (N–H str of CONH), 3090 (Ar–C–H str), 2946 (ali C–H str), 1648, 1565, 1478 (ali C–H def), 1352 (S=O str of SO_2NH, asymmetric), 1265 (S=O str of SO_2NH, symmetric), 1022, 980, 896 (Ar–C–H def)	7.96 (d, 2H, H–2', H–6'), 7.80 (d, 2H, H–3', H–5'), 7.62 (s, 1H, SO_2NH), 7.52 (m, 1H, CONH–1), 7.22 (m, 1H, CONH–5), 3.48 (m, 2H, N–CH–1''') 3.34 (m, 1H, H–2), 3.10 (m, 2H, N–CH_2–1''), 2.88 (m, 2H, CH_2 of Ar–i–Butyl), 2.70 (s, 1H, CH of Ar–i–Butyl), 2.52 (m, 2H, H_2–4) 1.82 (m, 2H, H_2–3), 1.76–1.58 (m, 6H, two CH_3 of Ar–i–Butyl), 1.33–1.16 (m, 8H, CH_2–2'', CH_2–3'', CH_2–2''', CH_2–3''') 0.92–0.72 (m, 6H, CH_3–4'', CH_3–4''')	60.90 61.08	8.67 8.67	9.26 9.13
31	M + H^+ peak at m/z 454	3362 (N–H str of CONH), 3094 (Ar–C–H str), 2948 (ali C–H str), 1652, 1568, 1482 (ali C–H def), 1355 (S=O str of SO_2NH, asymmetric), 1272 (S=O str of SO_2NH, symmetric), 1028, 982, 898 (Ar–C–H def)	7.98 (d, 2H, H–2', H–6'), 7.82 (d, 2H, H–3', H–5'), 7.56 (s, 1H, SO_2NH), 7.44 (m, 1H, CONH–1), 7.32 (m, 1H, CONH–5), 3.52 (m, 1H, H–2), 3.35 (m, 2H, N–CH_2–1'''), 3.14 (m, 2H, N–CH_2–1''), 2.96 (m, 2H, CH_2 of Ar–i–Butyl), 2.80 (s, 1H, CH of Ar–i–Butyl), 2.52 (m, 2H, H_2–4), 1.92 (m, 2H, H_2–3), 1.72–1.50 (m, 6H, two CH_3 of Ar–i–Butyl), 1.23–0.97 (m, 14H, CH–2'', CH–2''', CH_3–3'', CH_3–3''', CH_3–4'', CH_3–4''')	60.90 60.84	8.67 8.68	9.26 9.34
32	M + H^+ peak at m/z 494	3356 (N–H str of CONH), 3092 (Ar–C–H str), 2945 (ali C–H str), 1645, 1565, 1480 (ali C–H def), 1348 (S=O str of SO_2NH, asymmetric), 1270 (S=O str of SO_2NH, symmetric), 1021, 978, 894 (Ar–C–H def)	8.03 (s, 1H, SO_2NH), 7.78 (d, 2H, H–2', H–6'), 7.56 (d, 2H, H–3', H–5'), 7.06–6.77 (m, 10H, phenyl protons), 7.38–7.26 (m, 2H, CONH–1, CONH–5), 2.98 (m, 2H, CH_2 of Ar–i–Butyl), 2.82 (s, 1H, CH of Ar–i–Butyl), 2.72 (m, 1H, H–2), 2.44–2.33 (m, 4H, H_2–3, H_2–4), 1.70–1.52 (m, 6H, two CH_3 of Ar–i–Butyl)	65.70 65.62	6.33 6.35	8.51 8.46

Table 3. (Continued)

Cpd	Mass (FAB)	IR (KBr, cm^{-1})	^{1}HNMR (300 MHz, DMSO–d_6)	C,H,N: %calcd/found		
				C	H	N
33	$M + H^+$ peak at m/z 398	3354 (N–H str of CONH), 3084 (Ar–C–H str), 2938 (ali C–H str), 1642, 1560, 1474 (ali C–H def), 1346 (S=O str of SO_2NH, asymmetric), 1264 (S=O str of SO_2NH, symmetric), 1018, 972, 888 (Ar–C–H def)	7.88 (s, 1H, SO_2NH), 7.75 (d, 2H, H–2', H–6'), 7.64 (d, 2H, H–3', H–5'), 3.22 (m, 6H, CH_3–1''', CH_3–2'''), 3.12 (m, 1H, H–2), 2.94 (m, 2H, CH_2 of Ar–i–Butyl), 2.82 (m, 6H, CH_3–1'', CH_3–2''), 2.72 (s, 1H, CH of Ar–i–Butyl), 2.28 (m, 2H, H_2–4), 2.00 (m, 2H, H_2–3), 1.78–1.62 (m, 6H, two CH_3 of Ar–i–Butyl)	57.40 57.64	7.86 7.88	10.57 10.46
34	$M + H^+$ peak at m/z 507	3356 (N–H str of CONH), 3098 (Ar–C–H str), 2934 (ali C–H str), 1655, 1556, 1477 (ali C–H def), 1360 (S=O str of SO_2NH, asymmetric), 1272 (S=O str of SO_2NH, symmetric), 1022, 986, 896 (Ar–C–H def)	7.98 (d, 2H, H–2', H–6'), 7.73 (s, 1H, SO_2NH), 7.52 (d, 2H, H–3', H–5'), 7.32–7.22 (m, 2H, CONH–1, CONH–5), 2.90 (m, 2H, CH_2 of Ar–i–Butyl), 2.80 (s, 1H, CH of Ar–i–Butyl), 2.66 (m, 1H, H–2), 2.44–2.30 (m, 4H, H_2–3, H_2–4), 1.76–1.60 (m, 6H, two CH_3 of Ar–i–Butyl), 1.44–0.72 (m, 22H, cyclohexyl protons)	64.12 63.95	8.57 8.60	8.31 8.14
35	$M + H^+$ peak at m/z 511	IR (KBr, cm^{-1}): 3346 (N–H str of CONH), 3082 (Ar–C–H str), 2948 (ali C–H str), 1644, 1570, 1480 (ali C–H def), 1352 (S=O str of SO_2NH, asymmetric), 1267 (S=O str of SO_2NH, symmetric), 978, 892 (Ar–C–H def)	7.94 (d, 2H, H–2', H–6'), 7.76 (d, 2H, H–3', H–5'), 7.62 (s, 1H, SO_2NH), 6.88 (d, 1H, CONH–1), 6.56 (d, 1H, CONH–5), 3.42 (m, 2H, N–CH_2–1'''), 3.20–3.12 (m, 2H, N–CH_2–1''), 3.06 (m, 1H, H–2), 2.92 (m, 2H, CH_2 of Ar–i–Butyl), 2.82 (s, 1H, CH of Ar–i–Butyl), 2.70 (m, 2H, H_2–3), 2.18 (m, 2H, H_2–4), 1.82–1.58 (m, 16H, CH_2–2'', CH_2–2''', CH_2–3'', CH_2–3''', CH_2–4'', CH_2–4''', CH_2–5'', CH_2–5'''), 1.42–1.28 (m, 6H, two CH_3 of Ar–i–Butyl), 1.10–0.88 (m, 6H, CH_3–6'', CH_3–6''')	63.62 63.57	9.29 9.30	8.24 8.26
36	$M + H^+$ peak at m/z 370	3354 (N–H str of CONH), 3088 (Ar–C–H str), 2948 (ali C–H str), 1645, 1565, 1470 (ali C–H def), 1354 (S=O str of SO_2NH, asymmetric), 1269 (S=O str of SO_2NH, symmetric), 1024, 976, 894 (Ar–C–H def)	8.06 (s, 1H, SO_2NH), 7.90 (d, 2H, H–2', H–6'), 7.66 (d, 2H, H–3', H–5'), 3.34 (s, 1H, H–2), 2.40 (m, 2H, H_2–4), 2.32–2.28 (m, 2H, H_2–3), 2.14–1.88 (m, 9H, three CH_3 of t–Butyl), 1.40–1.26 (m, 12H, CH_3–1'', CH_3–2'', CH_3–1''', CH_3–2''')	55.26 55.42	7.37 7.35	11.37 11.44
37	$M + H^+$ peak at m/z 454	3344 (N–H str of CONH), 3080 (Ar–C–H str), 2944 (ali C–H str), 1645, 1567, 1482 (ali C–H def), 1350 (S=O str of SO_2NH, asymmetric), 1270 (S=O str of SO_2NH, symmetric), 1022, 978, 890 (Ar–C–H def)	8.02 (s, 1H, SO_2NH), 7.92 (d, 2H, H–2', H–6'), 7.56 (d, 2H, H–3', H–5'), 3.37 (s, 1H, H–2), 3.31–3.16 (m, 8H, N–CH_2–1'', N–CH_2–3'', N–CH_2–1''', N–CH_2–3'''), 2.43 (m, 2H, H_2–4), 2.28 (m, 2H, H_2–3), 2.10–1.82 (m, 9H, three CH_3 of t–Butyl), 1.41 (m, 6H, CH_3–2''', CH_3–4''') 1.32 (m, 6H, CH_3–2'', CH_3–4'')	60.90 61.13	8.67 8.66	9.26 9.32

2.2 Pharmacology

Twenty eight 1,5–*N*,*N*′–disubstituted–2–(substituted benzenesulphonyl) glutamamides (**10–37**) were biologically screened for their possible anticancer activity against Ehrlich Ascites Carcinoma (EAC) cells in Swiss Albino mice.

2.2.1 Tumor cells

Ehrlich Ascites Carcinoma (EAC) cells were originated from human breast carcinoma. EAC cells were maintained *in vivo* in Swiss Albino mice, by passaging every 10 days. EAC cells of 9 days old were used for the screening of the compounds (**10–37**).

2.2.2 Animals

Swiss albino mice of either sex of 10 weeks old with an average body weight of 18–20 grams were used. All mice were kept on basal metabolic diet with water *ad libitum*.

2.2.3 Screening protocol

Two groups of Swiss Albino Mice (each group contains 5 mice of the same sex, age and body weight) were selected at random and kept in two different cages under identical conditions. One of these two groups served as control while the other as test. Ehrlich Ascites Carcinoma (EAC) cells were collected from the donor mice and were suspended in sterile isotonic solution (0.9% w/v NaCl). The numbers of tumor cells per ml of this suspension were counted under microscope with the help of haemocytometer. A definite number (about 2×10^6 cells/0.2 ml) of these living viable cells were implanted into the peritoneal cavity of each mouse. In this instance, the tumor cells multiplied relatively freely within the peritoneal cavity and ascites developed. One day for incubation was allowed to establish the disease in the body before starting the drug administration. From the second day of transplantation up to the eighth day a suitable challenge dose (0.2 mmole/kg body weight) of the drug solution/suspension in sterile phosphate buffer (pH 7.2) was injected intraperitoneally to each mouse in the test group at 24 hr interval. Thus, seven doses of the drug were administered to each mouse in the test group. On the ninth day food and water was withheld 18 hr before the starting of the testing operation. The weights of all the animals were recorded before they were sacrificed. The peritoneal cavity was dissected, the fluid was sucked by adsorbent cotton and the weight of the 5 mice was recorded. The evaluation of the test drug was made by comparing tumor weight of the test with that of the control. The percentage inhibition of tumor weight was obtained by the following expression: Percentage inhibition of tumor weight = (1–T/C)×100, where T is the average weight of Ascitic fluid in test animals and C is the average weight of Ascites fluid in control animals. Anticancer activities of synthesized final compounds are shown in Table 4.

Table 4. Biological Activities of Glutamamide Analogues (**10–37**)

Cpd	R_1	R_2	R_3	R_4	R_5	%TWI (BA)	log BA
10	H	Cl	H	H	H	25.86	1.413
11	H	Cl	H	CH_3	H	21.43	1.331
12	H	Cl	H	C_2H5	H	35.29	1.548
13	H	Cl	H	*n*–C_3H_7	H	42.86	1.632
14	H	Cl	H	*i*–C_3H_7	H	52.58	1.721
15	H	Cl	H	*n*–C_4H_9	H	45.45	1.658
16	H	Cl	H	*i*–C_4H_9	H	32.50	1.512
17	H	Cl	H	CH3	CH3	41.66	1.620
18	H	Cl	H	C_6H_5	H	25.45	1.406
19	H	Cl	H	C_2H_5	C_2H_5	23.64	1.374
20	H	Cl	H	*n*–C_6H_{13}	H	40.11	1.603
21	Cl	H	Cl	H	H	14.67	1.166
22	Cl	H	Cl	CH3	H	20.83	1.319
23	Cl	H	Cl	*n*–C_3H_7	H	27.16	1.434
24	Cl	H	Cl	*c*–C_6H_{11}	H	31.87	1.503
25	H	*i*–C_4H_9	H	H	H	35.81	1.554
26	H	*i*–C_4H_9	H	CH_3	H	28.80	1.459
27	H	*i*–C_4H_9	H	C_2H_5	H	37.65	1.576
28	H	*i*–C_4H_9	H	*n*–C_3H_7	H	38.20	1.582
29	H	*i*–C_4H_9	H	*i*–C_3H_7	H	44.77	1.651
30	H	*i*–C_4H_9	H	*n*–C_4H_9	H	57.65	1.761
31	H	*i*–C_4H_9	H	*i*–C_4H_9	H	50.00	1.699
32	H	*i*–C_4H_9	H	C_6H_5	H	27.78	1.444
33	H	*i*–C_4H_9	H	CH_3	CH3	32.14	1.507
34	H	*i*–C_4H_9	H	*c*–C_6H_{13}	H	27.32	1.436
35	H	*i*–C_4H_9	H	*n*–C_6H_{13}	H	42.31	1.626
36	H	*t*–C_4H_9	H	CH_3	H	32.79	1.516
37	H	*t*–C_4H_9	H	C_2H_5	C_2H_5	34.02	1.532

2.3 QSAR Methodology

2.3.1 Dataset and parameters

All biologically evaluated compounds (**10–37**) were considered for the QSAR study. Logarithm of percentage inhibition of tumor weight [log BA] was taken as the biological activity parameter.

2.3.1.1 Electrotopological state atom (ETSA) indices

The E–state index [23–29] (S_i) of an atom *i* in a molecule is composed of an intrinsic state (I_i) and the perturbation effect (Δ_{ij}). The general expression of the intrinsic state of atom *i* in the N^{th} row of the periodic table is given as:

$$I_i = [((2/N)^2\delta^v + 1)/ \delta] \quad (1)$$

with δ^v = number of valence electron – number of hydrogen atom attached, and δ = number of sigma electron – number of hydrogen atom attached

The information encoded into the atom intrinsic value (I_i) is of both electronic and topological in nature. The count of π and lone pair electrons (δ^v) gives important electronic information because electrons occupying these orbitals are more reactive and closely associated with long–range non–

covalent intermolecular interaction such as drug–receptor encounters. The important topological attribute is the relative degree of mantle atom or buried atom status. This topological information is encoded by the number of skeletal neighbors (δ). The general expression for the perturbation effect is as follows:

$$\Delta_{ij} = \Sigma(I_i - I_j) / r_{ij}^2 \quad (2)$$

in which r_{ij} is the topological distance in the shortest path between the i^{th} and j^{th} atoms. Thus, the ETSA index (S_i) can be calculated as:

$$S_i = I_i + \Delta_{ij} \quad (3)$$

ETSA indices were calculated using the computer program 'Mouse' [31] developed in our laboratory. The program was written in the C++ language and can run in Windows operating system to calculate ETSA indices only. Before the calculation, the atoms of the molecules were numbered consecutively keeping the serial number of atoms same in all molecules. The intrinsic state (I_i) values of different atoms are then given as input and the output file represents the ETSA indices (S_i) of common atoms.

2.3.1.2 Refractotopological state atom (RTSA) indices

Molar refractivity is directly proportional to the polarizability of a substance. London force/dispersive force between two non–polar molecules has a direct relation to the polarizability. Thus, molecular refractivity is an important physicochemical property for modeling the dispersive/van der Waals interactions with the receptor. It is highly correlated with lipophilicity, molar volume and steric bulk. Ghosh *et al*. [32,33] reported the atomic contributions of molar refractivity. Keeping in view of these importance of molar refractivity and the successful application of ETSA index in many QSAR studies Carrasco *et al*. [34] introduced the refractotopological state atom (RTSA/R–state) index in the same way of ETSA index as defined by Kier and co–workers [35,36]. RTSA index is based on the atomic refractivity and the influences of other atoms in the chemical graph and its topological state. The same initial consideration of E–state formalism was taken for R−state index. The idea was that every atom in a molecule is present in a different information field composed of the other atoms of the molecule except where atoms mapped on to each other through a symmetry operation. The R–state index ($\mathcal{R}_i$) of an atom (i) in a molecule is composed of an intrinsic refractivity (AR_i) and the perturbation effect (ΔAR_i). The refractivity of the bonded hydrogen has been included to the non–hydrogen atoms connected to it as it was used to consider their contribution to the molar refractivity. The general expression for the perturbation effect is as follows:

$$\Delta AR_i = \Sigma(AR_i - AR_j) / r_{ij}^2 \quad (4)$$

where r_{ij} is the topological distance in the shortest path between the i^{th} and j^{th} atoms, Thus, the R−state index is calculated by the following expression:

$$\mathcal{R}_i = AR_i + \Delta AR_i \quad (5)$$

Atom–wise RTSA indices were calculated using the computer program 'Rat' [37] developed in our laboratory. The intrinsic refractivities for atoms are shown in the Table 5.

Table 5. Atomic Refractivity Values (AR) of Common Atoms

Atom type	Atomic Refractivity	Atom type	Atomic Refractivity
–F	1.0632	>C*=X [a]	3.0887
–Cl	5.6105	H	0.9155
–Br	8.6782	N_{sp3}	3.0100
–I	13.8741	N_{sp2}, N_{sp}	3.2009
–O–	1.6351	N^*O_2	3.5054
=O	1.7956	Ar–N*=X [a]	3.8095
O*=N	2.1407	N (Ar^b)	2.7662
C_{sp3}	2.8158	S_{sp3}	7.3190
C_{sp2}	3.8278	S_{sp2}	9.1680
C_{sp}	3.8974	$R–S^*O_2–R$	5.3321
C (Ar^b)	3.5090	R–S*O–R	6.0762

* Atomic refractivity of the corresponding atom; [a] Hetero atom; [b] Aromatic.

2.3.1.3 Physicochemical Parameters

Physicochemical parameters for the substituents like hydrophobicity (π), steric parameter (Es), Hammet's constant (σ) etc. were compiled from the literature [38]. Whole molecular descriptors such as molar refractivity, surface area, log P, mass and volume were calculated by HyperChem Professional software – version 7.0 of Hypercube Inc [39].

2.3.2 Correlation Analysis

Correlation analysis of ETSA indices, RTSA indices and physicochemical parameters was carried out. Autocorrelated parameters were eliminated stepwise depending on their individual correlation with the biological activity. All possible combinations of parameters were considered for multiple regression analysis.

2.3.3 Multiple Regression Analysis

Multiple regression analysis [40–43] was carried out by 'Multi Regress' [44] a program developed in our laboratory. The statistical quality of the regression equation were justified by parameters like correlation coefficient (R), percentage of explained variance (%EV), adjusted R^2 (R_A^2), variance ratio (F), standard error estimate (s). All the final equations have significant regression coefficients, intercepts and variance ratio (F) and that are more than 95% level. Use of more than one variable in the multivariate equation was justified by autocorrelation study.

2.3.4 Cross Validation

The predictive power of the equation is validated by Leave–One–Out (LOO) [45] cross–validation method. Predicted residual sum of square (*PRESS*), total sum of squares (*SSY*), cross–

validated R^2 (R_{cv}^2), standard error of *PRESS* (S_{PRESS}) and predictive standard error of prediction (S_{DEP}) for the QSAR equations are considered for the validation of the models.

Table 6. RTSA Indices, ETSA Indices, Physicochemical Parameters for QSAR Models

Cpd [a]	$\mathcal{R}_4$	$\mathcal{R}_{10}$	$\mathcal{R}_{14}$	$\mathcal{R}_{17}$	S_{10}	S_{11}	S_{13}	S_{14}	S_{17}	S_{av}	V [b]	EsR_4
10	2.296	4.016	3.989	3.820	2.131	–1.206	–0.156	–0.885	–0.650	–0.153	8.324	0.000
11	2.280	3.996	4.110	4.082	2.296	–1.040	0.025	–0.512	–0.277	0.098	8.994	–1.240
12	2.267	3.984	4.000	3.831	2.348	–1.035	0.040	–0.472	–0.238	0.129	9.695	–1.310
13	2.255	3.970	3.981	3.812	2.386	–1.034	0.049	–0.45	–0.216	0.147	10.727	–1.430
14	2.253	3.968	3.985	3.816	2.380	–1.060	0.025	–0.476	–0.242	0.125	11.233	–1.710
15	2.245	3.958	3.963	3.794	2.415	–1.034	0.054	–0.437	–0.202	0.159	11.937	–1.630
16	2.243	3.956	3.961	3.793	2.410	–1.053	0.037	–0.455	–0.220	0.144	13.283	–2.170
17	2.265	3.984	4.041	3.872	2.372	–1.025	0.055	–0.417	–0.182	0.161	12.251	–1.240
18	2.258	4.035	4.107	3.938	2.405	–1.170	–0.065	–0.567	–0.333	0.054	10.886	–1.010
19	2.237	3.952	4.011	3.842	2.475	–1.015	0.086	–0.337	–0.103	0.221	10.202	–1.310
20	2.228	3.939	3.935	3.766	2.457	–1.036	0.060	–0.421	–0.186	0.175	10.163	–1.540
21	4.799	4.005	3.976	3.811	2.079	–1.281	–0.195	–0.931	–0.679	–0.201	9.003	0.000
22	4.798	3.988	4.003	3.838	2.245	–1.115	–0.014	–0.559	–0.306	0.050	8.355	–1.240
23	4.797	3.959	3.968	3.803	2.335	–1.109	0.010	–0.497	–0.244	0.099	11.590	–1.430
24	4.815	3.971	3.999	3.834	2.463	–1.095	0.047	–0.421	–0.168	0.165	12.499	–1.810
25	2.256	3.998	3.973	3.808	2.214	–1.179	–0.136	–0.854	–0.630	–0.117	12.354	0.000
26	2.240	3.982	3.999	3.834	2.380	–1.013	0.046	–0.482	–0.257	0.135	11.275	–1.240
27	2.227	3.966	3.984	3.819	2.432	–1.008	0.061	–0.442	–0.218	0.165	10.661	–1.310
28	2.215	3.953	3.965	3.800	2.470	–1.006	0.069	–0.42	–0.196	0.183	11.296	–1.430
29	2.213	3.951	3.969	3.804	2.464	–1.033	0.046	–0.446	–0.222	0.162	10.812	–1.710
30	2.205	3.941	3.947	3.782	2.499	–1.007	0.075	–0.407	–0.182	0.196	10.180	–1.630
31	2.203	3.939	3.945	3.781	2.494	–1.025	0.058	–0.425	–0.200	0.180	10.273	–2.170
32	2.217	4.017	4.091	3.926	2.489	–1.143	–0.044	–0.537	–0.313	0.090	11.213	–1.010
33	2.224	3.966	4.025	3.861	2.455	–0.997	0.076	–0.386	–0.162	0.197	9.651	–1.240
34	2.200	3.964	3.995	3.830	2.599	–0.992	0.106	–0.344	–0.120	0.250	9.784	–1.810
35	2.188	3.921	3.919	3.754	2.541	–1.008	0.081	–0.39	–0.166	0.212	10.418	–1.540
36	2.295	3.980	3.997	3.833	2.378	–1.020	0.042	–0.486	–0.261	0.131	9.318	–1.240
37	2.252	3.932	3.993	3.829	2.558	–1.004	0.102	–0.311	–0.086	0.252	9.401	–1.310

[a] Compound number; [b] V is scaled by factor 0.01 to get linear relation with other parameters.

3 RESULTS AND DISCUSSION

3.1 Synthesis

1,5–*N*,*N*′–Disubstituted–2–(substituted benzenesulphonyl) glutamamides (**10**–**37**) were synthesized in accordance to Scheme 1. Detailed synthetic procedures are described in the Experimental part. Physical data of all intermediates and final compounds are presented in Tables 1 and 2, respectively. The yields of the title compounds were good, as shown in Table 2.

3.2 Anticancer activity

All final compounds (**10–37**) were biologically evaluated for their anticancer activity against Ehrlich Ascites Carcinoma (EAC) model in Swiss Albino mice. Percentage tumor weight inhibition (%TWI) of these compounds was determined at the dose level of 0.2 mmol/Kg body weight. Anticancer activities i.e., %TWI represented as the biological activity (BA) and the logarithmic value of the biological activity (log BA) of these final compounds are shown in Table 4.

3.3 QSAR study

Quantitative Structure–Activity Relationship study was performed on the anticancer activity of 1,5–*N*,*N*′–disubstituted–2–(substituted benzenesulphonyl) glutamamides (**10**–**37**) using electrotopological state atom (E–state) indices [23–29], refractotopological state atom (R–state) indices [30,31] and physicochemical parameters. E–state indices, R–state indices as well as physicochemical parameters of aliphatic substituents are presented in Table 6. Correlation analysis was performed using these independent parameters and the log of percentage of tumor weight inhibition (log BA) taking as the activity parameter. The correlation matrix of different parameters and log of biological activity is shown in Table 7.

Table 7. Correlation Matrix of Important Variables Used in QSAR Models

	S_{av}	S_{10}	S_{11}	S_{13}	S_{14}	S_{17}	$\mathcal{R}_4$	$\mathcal{R}_{10}$	$\mathcal{R}_{14}$	$\mathcal{R}_{17}$	V	EsR_4	log BA
S_{av}	1.00												
S_{10}	0.92	1.00											
S_{11}	0.92	0.76	1.00										
S_{13}	0.98	0.84	0.96	1.00									
S_{14}	0.99	0.88	0.90	0.98	1.00								
S_{17}	0.99	0.87	0.88	0.97	0.99	1.00							
$\mathcal{R}_4$	–0.36	–0.42	–0.51	–0.34	–0.31	–0.26	1.00						
$\mathcal{R}_{10}$	–0.71	–0.64	–0.71	–0.74	–0.68	–0.67	0.16	1.00					
$\mathcal{R}_{14}$	–0.12	–0.12	–0.21	–0.19	–0.08	–0.07	–0.05	0.72	1.00				
$\mathcal{R}_{17}$	–0.10	–0.15	–0.13	–0.13	–0.06	–0.06	–0.06	0.59	0.93	1.00			
V	0.19	0.24	0.09	0.15	0.19	0.19	–0.07	–0.12	–0.11	–0.19	1.00		
EsR_4	–0.84	–0.75	–0.74	–0.83	–0.85	–0.86	0.16	0.66	0.24	0.19	–0.33	1.00	
log BA	0.51	0.52	0.57	0.52	0.47	0.45	–0.52	–0.58	–0.47	–0.46	0.40	–0.53	1.00

Different possible combinations of these independent variables as suggested by the correlation study were used to develop QSAR models. The QSAR equations were developed in a stepwise fashion for modeling the antitumor activity using multiple linear regression analysis. Predictor variables with higher *p*–values were removed in developing QSAR models to get more acceptable QSAR models. The combination of R–state indices of atoms 4 and 10 ($\mathcal{R}_4$ and $\mathcal{R}_{10}$ respectively) yielded a QSAR model as follows:

$$\log BA = 11.517\ (\pm 2.735) - 0.064\ (\pm 0.021)\ \mathcal{R}_4 - 2.475\ (\pm 0.691)\ \mathcal{R}_{10}$$
$$n = 28 \quad R = 0.720 \quad \%EV = 0.517 \quad R_A^2 = 0.478 \quad F_{(2,25)} = 13.386 \quad p<0.000 \quad s = 0.097 \qquad (6)$$
$$PRESS = 0.293 \quad SSY = 0.488 \quad R_{cv}^2 = 0.400 \quad S_{PRESS} = 0.108 \quad S_{DEP} = 0.102$$

where n is the number of data points, R is correlation coefficient. $\%EV$, R_A^2, F, p, s, $PRESS$, SSY, R_{cv}^2, S_{PRESS} and S_{DEP} are percentage of explained variance, adjusted R^2, ratio between the variances of observed and calculated activities, probability factor related to F–ratio, standard error of estimate, predicted residual sum of squares, total sum of squares, cross validated R^2 and standard error of prediction respectively. Quantities in parenthesis are the standard error of the corresponding parameters.

Eq. (6) explains up to 51.70% of the variances in the activity data. Negative coefficients of $\mathcal{R}_4$

and $\mathcal{R}_{10}$ in the equation suggest that lower values of these indices are advantageous to the activity and atoms 4 and 10 might play crucial role in the dispersive/van der Waals interaction with the receptor surface. Another combination of R–state indices of atoms 4 and 17 ($\mathcal{R}_4$ and $\mathcal{R}_{17}$ respectively) gave the following equation:

$$\log BA = 5.786\ (\pm 1.137) - 0.081\ (\pm 0.020)\ \mathcal{R}_4 - 1.058\ (\pm 0.296)\ \mathcal{R}_{17}$$
$$n = 28 \quad R = 0.720 \quad \%EV = 0.517 \quad R_A^2 = 0.478 \quad F_{(2,25)} = 13.371 \quad p<0.000 \quad s = 0.097 \qquad (7)$$
$$PRESS = 0.322 \quad SSY = 0.488 \quad R_{cv}^2 = 0.340 \quad S_{PRESS} = 0.113 \quad S_{DEP} = 0.107$$

The QSAR Eq. (7) explains up to 51.70% of the variances in the antitumor activity. The equation signifies the importance of another atom i.e. atom 17 in interacting with the receptor(s) through dispersive force.

The best bi–variate relation was obtained when the combination of R–state indices of atoms 4 and 14 ($\mathcal{R}_4$ and $\mathcal{R}_{14}$ respectively) was taken as independent parameters. The resultant equation is shown as

$$\log BA = 7.552\ (\pm 1.602) - 0.080\ (\pm 0.020)\ \mathcal{R}_4 - 1.458\ (\pm 0.400)\ \mathcal{R}_{14}$$
$$n = 28 \quad R = 0.723 \quad \%EV = 0.522 \quad R_A^2 = 0.484 \quad F_{(2,25)} = 13.676 \quad p<0.000 \quad s = 0.097 \qquad (8)$$
$$PRESS = 0.313 \quad SSY = 0.488 \quad R_{cv}^2 = 0.359 \quad S_{PRESS} = 0.112 \quad S_{DEP} = 0.106$$

The explained variance and predicted variance of the Eq. (8) are 52.20% and 48.40% respectively. The negative coefficient of $\mathcal{R}_{14}$ (R–state index of atom 14) in Eq. (8) encodes that lower value of this index will increase the antitumor activity of glutamamides. When steric term (EsR_4) at the R_4 position was considered along with the R–state indices of atoms 4 and 14 ($\mathcal{R}_4$ and $\mathcal{R}_{14}$ respectively) a better model was obtained which is shown in the QSAR Eq. (9):

$$\log BA = 6.394\ (\pm 1.491) - 0.071\ (\pm 0.018)\ \mathcal{R}_4 - 1.202\ (\pm 0.369)\ \mathcal{R}_{14} - 0.087\ (\pm 0.032)\ EsR_4$$
$$n = 28 \quad R = 0.797 \quad \%EV = 0.636 \quad R_A^2 = 0.590 \quad F_{(3,24)} = 13.952 \quad p<0.000 \quad s = 0.086 \qquad (9)$$
$$PRESS = 0.256 \quad SSY = 0.488 \quad R_{cv}^2 = 0.475 \quad S_{PRESS} = 0.103 \quad S_{DEP} = 0.096$$

The negative contribution of EsR_4 in Eq. (9) suggests that the steric bulk at R_4 substitution is slightly advantageous to the antitumor activity of glutamamides. Eq. (9) explains up to 63.60% of the variances in the antitumor activity. When combination of R–state indices of atoms 4 and 14 ($\mathcal{R}_4$ and $\mathcal{R}_{14}$ respectively) and molar volume (V) were used the following equation was developed:

$$\log BA = 6.983\ (\pm 1.375) - 0.079\ (\pm 0.017)\ \mathcal{R}_4 - 1.437\ (\pm 0.339)\ \mathcal{R}_{14} + 0.046\ (\pm 0.014)\ V$$
$$\text{DC} = \mathbf{16} \quad n = 27 \quad R = 0.832 \quad \%EV = 0.693 \quad R_A^2 = 0.653 \quad F_{(3,23)} = 17.283 \quad p<0.000 \qquad (10)$$
$$s = 0.081 \quad PRESS = 0.212 \quad SSY = 0.488 \quad R_{cv}^2 = 0.566 \quad S_{PRESS} = 0.096 \quad S_{DEP} = 0.089$$

where DC is the deleted compound behaves as outlier, might act through a different mechanism of action. Eq. (10) explains 69.30% of the variances in the activity. The positive regression coefficient of molar volume in Eq. (10) suggests that the increased molar volume (V) of glutamamide analogues may contribute to higher anticancer activity.

Table 8. *t*–Statistics and p–Values of Intercepts and Different Parameters

Eq.	Intercepts/ Parameters	*t*–values	*p*–values	Eq	Intercepts/ Parameters	*t*–values	*p*–values
6	Intercept	4.211	0.000	**10**	Intercept	5.079	0.000
	$\mathcal{R}_4$	–3.100	0.005		$\mathcal{R}_4$	–4.637	0.000
	$\mathcal{R}_{10}$	–3.583	0.001		$\mathcal{R}_{14}$	–4.239	0.000
					V	3.397	0.002
7	Intercept	5.087	0.000				
	$\mathcal{R}_4$	–3.943	0.000	**11**	Intercept	5.023	0.000
	$\mathcal{R}_{17}$	–3.580	0.001		S_{av}	1.904	0.070*
					$\mathcal{R}_4$	–3.838	0.001
8	Intercept	4.712	0.000		$\mathcal{R}_{14}$	–4.160	0.000
	$\mathcal{R}_4$	–3.947	0.001		V	3.186	0.004
	$\mathcal{R}_{14}$	–3.642	0.001				
				12	Intercept	5.419	0.000
9	Intercept	4.289	0.000		S_{av}	2.569	0.018
	$\mathcal{R}_4$	–3.873	0.001		$\mathcal{R}_4$	–4.322	0.000
	$\mathcal{R}_{14}$	–3.258	0.003		$\mathcal{R}_{14}$	–4.427	0.000
	EsR_4	–2.729	0.012		V	3.361	0.003

*Regression coefficient is less than 95% confidence interval.

Attempt was made to find if ETSA indices could be used along with $\mathcal{R}_4$ and $\mathcal{R}_{14}$ (R–state indices of atoms 4 and 14 respectively) as well as molar volume. From the correlation analysis it was found that ETSA indices of atoms 10, 11, 13, 14 and 17 (S_{10}, S_{11}, S_{13}, S_{14} and S_{17} respectively) were highly autocorrelated. These indices cannot be used in the same QSAR model. But omitting any of these indices might loose some information at atomic/fragmental level regarding the anticancer activity of this type of compounds. To accommodate these indices, an average of these indices (S_{av}) was taken as the single best non auto–correlated variable. The following QSAR model was developed using S_{av} (average of ETSA indices of atoms 10, 11, 13, 14 and 17) as an independent variable:

$$\begin{aligned} \log \mathrm{BA} = {} & 6.615\ (\pm 1.317) + 0.279\ (\pm 0.147)\ S_{av} - 0.067\ (\pm 0.017)\ \mathcal{R}_4 \\ & - 1.350\ (\pm 0.324)\ \mathcal{R}_{14} + 0.042\ (\pm 0.013)\ V \\ \mathrm{DC} = \mathbf{16} \quad & n = 27 \quad R = 0.858 \quad \%EV = 0.736 \quad R_A^2 = 0.688 \quad F_{(4,22)} = 15.348 \quad p<0.000 \\ s = 0.076 \quad & PRESS = 0.183 \quad SSY = 0.488 \quad R_{cv}^2 = 0.625 \quad S_{PRESS} = 0.091 \quad S_{DEP} = 0.082 \end{aligned} \tag{11}$$

From the equation it is revealed that atoms 10, 11, 13, 14 and 17 may have important contribution to the electronic interaction with the receptor(s) surface. Positive regression coefficient of S_{av} (average of ETSA indices of atoms 10, 11, 13, 14 and 17) in the Eq. (11) suggests that higher values of this index are conducive to the better anticancer activity of glutamamide analogues. Explained variance and predicted variance of the Eq. (11) are 73.60% and 68.80% respectively.

Table 9. Observed (Obs), Calculated (Calc), Residual (Res), LOO–predicted (Pred) and Predicted Residual (Pres) Values of Eq. (12).

Cpd	Obs	Calc	Res	Pred	Pres
10	1.413	1.379	0.033	1.355	0.057
11	1.331	1.337	–0.006	1.341	–0.009
12	1.548	1.518	0.030	1.516	0.032
13	1.632	1.590	0.042	1.588	0.044
14	1.721	1.598	0.123	1.589	0.132
15	1.658	1.666	–0.008	1.667	–0.009
16	1.512	–	–	–	–
17	1.620	1.577	0.042	1.568	0.052
18	1.406	1.402	0.003	1.401	0.005
19	1.374	–	–	–	–
20	1.603	1.638	–0.035	1.643	–0.040
21	1.166	1.238	–0.071	1.301	–0.135
22	1.319	1.263	0.055	1.230	0.089
23	1.434	1.453	–0.019	1.462	–0.028
24	1.503	1.471	0.032	1.446	0.057
25	1.554	1.574	–0.020	1.592	–0.038
26	1.459	1.585	–0.126	1.594	–0.135
27	1.576	1.591	–0.016	1.592	–0.017
28	1.582	1.648	–0.066	1.654	–0.072
29	1.651	1.617	0.034	1.615	0.036
30	1.761	1.632	0.129	1.617	0.143
31	1.699	1.633	0.066	1.626	0.073
32	1.444	1.451	–0.007	1.453	–0.009
33	1.507	1.510	–0.003	1.510	–0.003
34	1.436	1.573	–0.137	1.593	–0.156
35	1.626	1.684	–0.058	1.695	–0.069
36	1.516	1.505	0.010	1.504	0.011
37	1.532	1.558	–0.026	1.563	–0.031

Compound (**19**) also behaves as an outlier with larger residual. It might act through different mechanism of action. Exclusion of the compound (**19**) in Eq. (12) improved the statistical significance as well as the predictive power as shown:

$$\begin{gathered}\log \mathrm{BA} = 6.383\ (\pm 1.178) + 0.342\ (\pm 0.133)\ S_{\mathrm{av}} - 0.067\ (\pm 0.016)\ \mathcal{R}_4 \\ - 1.285\ (\pm 0.290)\ \mathcal{R}_{14} + 0.040\ (\pm 0.012)\ V \\ \mathrm{DC} = \mathbf{16}, \mathbf{19} \quad n = 26 \quad R = 0.889 \quad \%EV = 0.790 \quad R_A^2 = 0.750 \quad F_{(4,21)} = 19.749 \quad p<0.000 \\ s = 0.068 \quad PRESS = 0.141 \quad SSY = 0.465 \quad R_{cv}^2 = 0.697 \quad S_{PRESS} = 0.082 \quad S_{DEP} = 0.07\end{gathered} \tag{12}$$

where DC is the deleted compound behaves as outlier. Eq. (12) explains up to 79.00% of the variances in the antitumor activity. The values within the parenthesis are more than 95% confidence interval as supported by the *t*–statistics and *p*–values. The student *t*–values and probability–*p* values of all the equations are given in Table 8.

The lower value of S_{PRESS} in Eq. (12) suggests that the optimum numbers of variables are taken for the generation of the QSAR model. The predictive power of the final equation, Eq. (12), was confirmed by LOO–cross–validation method where one compound is deleted at once and prediction of the activity of the deleted compound is made based on the QSAR model. The process is repeated after elimination of another compound until all of the compounds have been deleted at once. The observed (Obs), calculated (Calc), LOO– predicted (Pred) and predicted residual (Pres) values of

the final Eq. (12) is shown in Table 9.

4 CONCLUSIONS

The study showed the importance of the particular atoms and identified a functional region of the molecule with the potential as the pharmacophore. This is shown in Figure 3. RTSA indices $\mathcal{R}_4$ and $\mathcal{R}_{14}$ (RTSA indices of atoms 4 and 14 respectively) were used to generate the final QSAR Eq. (7). The RTSA indices are related with the atomic refractivity as well as the molecular connection and are measures of the dispersive/van der Waals force between two non–polar molecules. Thus, the atoms 4 and 14 may be essential for the receptor(s) surface and are important for dispersive interactions with the receptor(s). ETSA index S_{av} (average of ETSA indices of atoms 10, 11, 13, 14 and 17) is also useful to generate statistically significant QSAR Eq. (12). Since ETSA indices are the measure of the availability of the π and / or lone pair electrons on the atoms it is evident that atoms 10, 11, 13, 14 and 17 may play some electronic roles in the interaction of this type of compounds with the receptor(s).

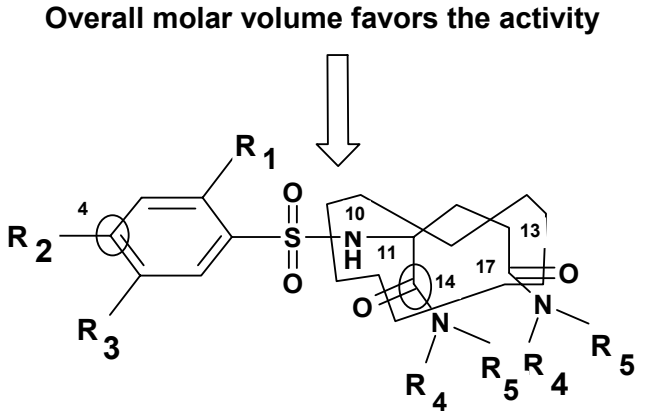

Figure 3. Pharmacophoric requirements of glutamamide analogues for the antitumor activity. Atoms bounded by circle are important for dispersive interaction with the receptor(s) and atoms bounded by straight lines are important for electronic interaction with the receptor(s).

These atoms may constitute the pharmacophore associated with the electronic interaction. Besides, increased molar volumes of these analogues have advantageous effect to the anticancer activity. These features may be helpful for further synthesis of better active glutamamide analogues as the anticancer agents in future.

Acknowledgment

Authors are thankful to the University Grants Commission (UGC), New Delhi and All India Council for Technical Education (AICTE), New Delhi for providing financial support to the research work. Two of the authors SG and SS are grateful to UGC, New Delhi for awarding Post–Graduate Fellowship and Junior Research Fellowship (JRF) respectively. Another author BD is indebted to the Council for Scientific and Industrial Research (CSIR), New Delhi for providing a Senior Research Fellowship (SRF). Authors are also grateful to the authority of Jadavpur University for providing research facilities.

5 REFERENCES

[1] M. Medina, Glutamine and cancer, *J. Nutr*. **2001**, *131*, 2539S–2542S.
[2] V. S. Klimberg and J. L. McClellan, Glutamine, cancer, and its therapy, *Am. J. Surg*. **1996**, *172*, 418–424.
[3] C. Costa, J. F. Huneau and D. Tome, Characteristics of L–glutamine transport during Caco–2 cell differentiation, *Biochem. Biophys. Acta/Biomemb*. **2000**, *1509*, 95–102.
[4] H. Zalkin and J. L. Smith, Enzymes utilizing glutamine as an amide donor, *Adv. Enzymol. Relat. Areas. Mol. Biol*. **1998**, *72*, 87–144.
[5] F. Massiere and M. A. Badet–Denisot, The mechanism of glutamine–dependent amidotransferases, *Cell Mol. Life Sci*. **1998**, *54*, 205–222.
[6] L. Kallinowski, S. Runkel, H. P. Fortmeyer, H. Forster and P. Vaupel, L–glutamine: a major substrate for tumor cells in vivo? *Cancer Res. Clin. Oncol*. **1987**, *113*, 209–215.
[7] Y. J. Kang, Y. Feng and E. L. Hatcher, Glutathione stimulates A549 cell proliferation in glutamine–deficient culture: the effect of glutamate supplementation, *J. Cell. Physiol*. **1994**, *161*, 589–596.
[8] Y. J. Kang, Buthionine sulfoximine spares intracellular glutamate: a possible mechanism for cell growth stimulation, *Cell. Mol. Biol. Res*. **1993**, *39*, 675–684.
[9] G. Ollenschlager, A. Simmel and E. Roth, Availability of glutamine from peptides and acetylglutamine for human tumor–cell cultures, Metabolism, **1989**, *38*, 40–42.
[10] C. L. Collins, M. Wasa,; W. W. Sauba and S. F. Abcouwer, Determinants of glutamine dependence and utilization by normal and tumor–derived breast cell lines, *J. Cell. Physiol*. **1998**, *176*, 166–178.
[11] A. Colquhonn and E. A. Newsholme, Aspects of glutamine metabolism in human tumour cells, *Biochem. Mol. Biol. Int*. **1997**, *41*, 583–596.
[12] M. Wasa, B. P. Bode, S. F. Abcouwer, C. L. Collins, K. K. Tanabe and W. W. Souba, Glutamine as a regulator of DNA and protein biosynthesis in human solid tumor cell lines, *Ann. Surg*. **1996**, *224*, 189–197.
[13] S. D. Lyons, M. E. Sant and R. I. Christopherson, Cytotoxic mechanisms of glutamine antagonists in mouse L1210 leukemia, *J Biol Chem*. **1990**, *265*, 11377–11381.
[14] S. K. Purkayastha, T. Jha, D. K. Pal and A. U. De, Possible antineoplastic agents: Part XIII. Synthesis, biological evaluation and QSAR studies of some 1–(substituted benzenesulphonyl)–5–oxopyrrolidine–2–carboxylic acid derivatives, *Anticancer Drug Des*. **1993**, *8*, 95–100.
[15] T. Jha, In Frontiers of Pharmaceutical Technology, J. K. Gupta, T. Jha, Eds., Jadavpur University: Calcutta, 1999, pp87–96.
[16] K. Srikanth, C. A. Kumar, D. Goswami, A. U. De and T. Jha, Quantitative structure activity relationship (QSAR) studies of some substituted benzenesulphonyl glutamines as tumour suppressors, *Ind. J. Biochem. Biophys*. **2001**, *38*, 120–123.
[17] K. Srikanth, B. Debnath and T. Jha, Synthesis, biological evaluation and QSAR study on antitumor activity of 1,5–*N*,*N*′–disubstituted–2–(substituted benzenesulphonyl) glutamamides, *Bioorg. Med. Chem*. **2002**, *10*, 1841–1854.
[18] K. Srikanth, C. A. Kumar, B. Ghosh and T. Jha, Synthesis, screening and quantitative structure–activity relationship (QSAR) studies of some glutamine analogues for possible anticancer activity, *Bioorg. Med. Chem*. **2002**, *10*, 2119–2131.
[19] B. Debnath, K. Srikanth, S. Banerjee and T. Jha, 1,5– *N*,*N*′–Disubstituted–2–(substituted benzenesulphonyl)–glutamamides as antitumor agents. Part 2. synthesis, biological activity and QSAR study, *Internet Electron. J. Mol. Des*. **2002**, *1*, 488–502. www.biochempress.com
[20] T. Jha, B. Debnath, S. Samanta and A. U. De, QSAR study on some substituted glutamine analogs as anticancer agents, *Internet Electron. J. Mol. Des*. **2003**, *2*, 539–545. www.biochempress.com
[21] K. Srikanth, B. Debnath and T. Jha, QSAR study on adenosine kinase inhibition of pyrrolo[2,3–d] pyrimidine nucleoside analogs using Hansch approach, *Bioorg. Med. Chem. Lett*. **2002**, *12*, 899–902.
[22] B. Debnath, S. P. Vishnoi, B. Sa and T. Jha, QSAR study on some dihydrofolate reductase inhibitors, *Internet Electron. J. Mol. Des*. **2003**, *1*, 128–136. www.biochempress.com
[23] B. Debnath, S. Samanta, K. Roy and T. Jha, QSAR study on some p–arylthio cinnamides as antagonists of biochemical ICAM–1/LFA–1 interaction and ICAM–1/JY–8 cell adhesion in relation to anti–inflammatory activity, *Bioorg. Med. Chem*. **2003**, *11*, 1615–1619.
[24] B. Debnath, S. Samanta, S. K. Naskar, K. Roy and T. Jha, study on the affinity of some arylpiperazines towards the 5–HT1A/alpha1–adrenergic receptor using the E–state index, *Bioorg. Med. Chem. Lett*. **2003**, *13*, 2837–2842.
[25] B. Debnath, S. Gayen, S. K. Naskar, K. Roy and T. Jha, QSAR study of some azidopyridinyl neonicotinoids insecticides for their selective affinity towards the Drosophilla nicotinic receptor over mammalian $\alpha_4\beta_2$ receptor using electrotopological state atom index, *Drug Des. Discov*. **2003**, *18*, 81–89.
[26] B. Debnath, S. Gayen, S. Bhattacharya, S. Samanta and T. Jha, QSAR study on some pyridoacridine ascididemin

analogs as anti–tumor agents, *Bioorg*. *Med*. *Chem*. **2003**, *11*, 5493–5499.
[27] S. Samanta, K. Srikanth, S. Banarjee, B. Debnath, S. Gayen and T. Jha, 5–N–Substituted–2–(substituted benzenesulphonyl) glutamines as antitumor agents II: synthesis, biological activity and QSAR study, *Bioorg*. *Med*. *Chem*. **2004**, *12*, 1413–1423.
[28] S. Gayen, B. Debnath, S. Samanta and T. Jha, QSAR study on some anti–HIV HEPT analogues using physicochemical and topological parameters, *Bioorg*. *Med*. *Chem*. **2004**, *12*, 1493–1503.
[29] B. Debnath, S. Gayen, A. Basu, K. Srikanth and T. Jha, Quantitative structure–activity relationship study on some benzodiazepine derivatives as anti–Alzheimer agents. *J*. *Mol*. *Mod*. **2004**, *10*, 328–334.
[30] B. Debnath, S. Gayen, A. Basu, B. Ghosh, K. Srikanth and T. Jha, Quantitative Structure–Activity Relationship Study Using Refractotopological State Atom Index on Some Neonicotinoid Insecticides, *Bioorg*. *Med*. *Chem*. **2004**, *12*, 6137–6145.
[31] Mouse, a computer program written in C^{++} language by S. K. Naskar of Department of Computer Science and Engineering, Jadavpur University and B. Debnath, one of the authors of this article.
[32] A. K. Ghose, A. Pritchett and G. M. Crippen, Atomic physicochemical parameters for three dimensional structure directed quantitative structure–activity relationships III: modeling hydrophobic interactions, *J*. *Comp*. *Chem*. **1988**, *9*, 80–90.
[33] A. K. Ghose and G. M. Crippen, Atomic physicochemical parameters for three–dimensional–structure–directed quantitative structure–activity relationships. 2. Modeling dispersive and hydrophobic interactions *J*. *Chem*. *Inf*. *Comput*. *Sci*. **1987**, *27*, 21–35.
[34] R. Carrasco, J. A. Padron and J. J. Galvez, Definition of a novel atomic index for QSAR: The refractotopological state, *Pharm*. *Pharmaceut*. *Sci*. **2004**, *7*, 19–26.
[35] L. B. Kier and L. H. Hall, An electrotopological–state index for atoms in molecules, *Pharm*. *Res*. **1990**, *7*, 801–807.
[36] K. Rose, L. H. Hall and L. B. Kier, Modeling blood–brain barrier partitioning using the electrotopological state, *J*. *Chem*. *Inf*. *Comput*. *Sci*. **2002**, *42*, 651–666.
[37] Rat, a computer programme written in C^{++} language by B. Debnath and S. Gayen, authors of this article.
[38] C. Hansch and A. Leo, *Substituent constants for correlation analysis in chemistry and biology*, **1979**, John Wiley & Sons: NY, pp 48–63.
[39] HyperChem Professional' software – version 7.0 of Hypercube Inc. www.hyper.com
[40] G G. W. Snedecor and W.G. Cochran, *Statistical Methods*; Oxford & IBH: New Delhi, 1967, pp. 381.
[41] J. O. Rawlings, *Applied Regression Analysis*; Wardsworth: CA, USA, 1988, pp. 327.
[42] N. R. Darper and H. Smith, *Applied Regression Analysis*, John Wiley & Sons: New York, 1981, pp. 294.
[43] E. J. Lien, In *Quantitative Correlations Using Multiple Regression and Substituent Constants*; E. J. Ariens, Drug Design; Academic: New York, 1975; Vol. V, pp. 84..
[44] Multiregress, a computer program written in C^{++} language by S. K. Naskar of Department of Computer Science and Engineering, Jadavpur University and B. Debnath, one of the authors of this article.
[45] I. V. Tetko, V. Y Tanchuk and A. E. Villa, Prediction of n–octanol/water partition coefficients from PHYSPROP database using artificial neural networks and E–state indices, *J*. *Chem*. *Inf*. *Comput*. *Sci*. **2001**, *41*, 1407–1421.